Technical Control and Optimal Dispatch Strategy for a Hybrid Energy System

Laetitia Uwineza [1,2] , Hyun-Goo Kim [1,]* , Jan Kleissl [3] and Chang Ki Kim [1]

[1] New and Renewable Energy Resource Map Laboratory, Korea Institute of Energy Research,
Daejeon 34129, Korea; uwinezalaetitiamary@gmail.com (L.U.); ckkim@kier.re.kr (C.K.K.)

[2] Department of Renewable Energy Engineering, University of Science and Technology, Daejeon 34113, Korea

[3] Center for Energy Research, University of California San Diego, La Jolla, CA 92093, USA;
jkleissl@eng.ucsd.edu

* Correspondence: hyungoo@kier.re.kr

Abstract: Optimal dispatch is a major concern in the optimization of hybrid energy systems (HESs). Efficient and effective dispatch models that satisfy the load demand at the minimum net present cost (NPC) are crucial because of the high capital costs of renewable energy technologies. The dispatch algorithms native to hybrid optimization of multiple energy resources (HOMER) software, cycle-charging (CC) and load-following (LF), are powerful for modeling and optimizing HESs. In these control strategies, the decision to use fuel cell systems (FCs) or battery energy storage systems (BESs) at each time step is made based on the lowest cost choice. In addition, the simultaneous operation of a FC with a BES reduces the operating efficiency of the FC. These deficiencies can affect the optimal design of HESs. This study introduces a dispatch algorithm specifically designed to minimize the NPC by maximizing the usage of FCs over other components of HESs. The framework resolves the dispatch deficiencies of native HOMER dispatch algorithms. The MATLAB Version 2021a, Mathworks Inc., Natick, MA, USA Link feature in HOMER software was used to implement the proposed dispatch (PD) algorithm. The results show that the PD achieved cost savings of 4% compared to the CC and LF control dispatch strategies. Furthermore, FCs contributed approximately 23.7% of the total electricity production in the HES, which is more than that of CC (18.2%) and LF (18.6%). The developed model can be beneficial to engineers and stakeholders when optimizing HESs to achieve the minimum NPC and efficient energy management.

Keywords: control dispatch strategy; optimization; microgrid system; net present cost

1. Introduction

The deployment of renewable energy has proven to be essential for the decarbonization of energy systems. Electricity is primarily produced by large centralized power plants operated by traditional fossil fuel generators [1]. However, this increases greenhouse gas emissions and transmission losses owing to the long distances between power generation centers and distribution systems [2,3]. Microgrid systems (grid-connected or islanded modes) have been suggested over the years to mitigate such problems because they use locally available renewable energy sources and battery energy storage systems (BESs) to satisfy local load demand levels. These hybrid energy systems (HESs) can reduce the consumption of fossil fuels and mitigate the high price of electricity from the main grid [4]. The main challenge when designing a HES is the choice of the best optimization model and control dispatch strategy to ensure the proper size of the microgrid components and to make the system reliable, efficient, and cost effective [5].

Several studies have attempted to size HESs by applying different control dispatch strategies and optimization models [6]. HOMER is one of the most commonly used simulation models for the design of the microgrid systems [7]. HOMER determines the optimal design to satisfy load demand levels based on the lowest total net present cost (NPC) [8].

This software offers several dispatch options for HESs, such as cycle-charging (CC), load-following (LF), and user-defined control dispatch strategies that can be developed using the MATLAB Version 2021a, Mathworks Inc., Natick, MA, USA Link feature. In the LF strategy, the diesel generator (DG) operates to exactly meet (load follow) the power demand without charging the BES; the BES is only charged using renewable energy. However, whenever it is required to run, the DG in the CC strategy runs at the full-rated power to meet the power demand and charge the BES using surplus electrical production [9]. Therefore, the LF strategy is designed to maximize renewable energy self- consumption, whereas the CC strategy is designed to maximize reliability.

Several valuable papers have been reviewed in which the native HOMER CC and LF control strategies have been adopted for different HESs based on photovoltaic systems (PVs) and fuel cell systems (FCs). Recently, Dawood et al. [10] applied the LF control dispatch of a hybrid system consisting of a PV, BES, and FC, including hydrogen storage, in an effort to minimize the NPC using HOMER. The results showed that the LF control strategy permits the BES to discharge electricity while the FC supplies the load, which may cause the FC to run under partial power, resulting in a low operating efficiency. Singh et al. [11] presented a PV, BES, and FC HES to meet the electric load and thermal load demands with the objective of minimizing the NPC using CC control dispatch. The results showed that the FC is operated at the maximum capacity to meet the load demand, and that surplus power is used to run the electrolyzer (EL) for hydrogen production and to charge the BES. However, the BES can only start discharging at the maximum SOC [12].

Other studies have compared the abilities of CC and LF control strategies to optimally size a HES. Kansara and Parekh [13] assessed the performance of a microgrid system consisting of wind turbines and a DG using both CC and LF control strategies in HOMER. The results showed that the LF strategy reduced the NPC for high renewable penetration compared to the CC control dispatch. In Ref. [14], the authors studied the techno-economic sizing of PVs, wind turbines, hydrokinetic turbines, BESs, and DGs using the CC and LF control algorithms. The LF control strategy achieved cost savings compared to the CC control dispatch. Shoeb and Shafiullah [15] found that the CC strategy provided a more economical optimum design than the LF strategy in the off-grid PV, DG, and BES cases in Southern Bangladesh. Arévalo and Jurado [16] presented a study to evaluate the techno-economic feasibility of a PV–hydrokinetic turbine–wind turbine–DG hybrid autonomous grid for a campus building in Southern Ecuador, where LF and CC were used as control dispatches. The results showed that the LF control strategy reduced the NPC and levelized cost of energy (LCOE) when using an energy storage system composed of pumped hydro. Table 1 summarizes other studies on HESs using LF, CC, and user-defined control dispatch in HOMER. Certain studies have reported that the CC and LF strategies are inferior to other proposed control dispatch strategies in terms of both LCOE and NPC.

Table 1. Literature review of hybrid energy studies using different HOMER and custom dispatch strategies.

Reference	Year	Generator Technology	Dispatch Strategy	Optimization Models	Site	Results
Rezzouk et al. [17]	2015	PV/BES/DG	LF	HOMER	North Algeria	Increasing renewable energy reduces energy cost.
Yilmaz et al. [18]	2017	PV/BES/DG	LF and CC	HOMER	Turkey	HOMER sizing results are sensitive to the optimization model.
Rajbongshi et al. [19]	2017	PV/Biomass DG/BES/Grid	CC	HOMER	India	Grid-connected system had a lower LCOE than the off-grid system.

Table 1. *Cont.*

Reference	Year	Generator Technology	Dispatch Strategy	Optimization Models	Site	Results
Rashid et al. [20]	2019	PV/BES/DG	LF, CC, and custom dispatch	HOMER + GA	Bangladesh	The proposed control dispatch yields higher economical and performance benefits than LF and CC.
Arévalo et al. [21]	2020	PV/BES/hydro-kinetic	LF, CC, and custom dispatch	HOMER + MATLAB	Ecuador	The proposed dispatch reduces NPC and LCOE compared to LF.
Ghorbani et al. [22]	2018	PV/BES /wind turbines	LF and custom dispatch	GAPSO/MOPSO + HOMER	Iran	GAPSO/MOPSO algorithm improves over HOMER.
Fodhil et al. [23]	2019	PV/BES/DG	LF and CC	HOMER + PSO	Algeria	PSO is more cost effective than CC and LF control strategy.
Arévalo et al. [24]	2022	PV/BES/wind turbines/hydro-electric storage	Energy control models	HOMER+ MATLAB	Galapagos Islands	Increasing PV capacity and pumped hydraulic storage reduces LCOE.
Emad et al. [25]	2021	PV/BES/wind turbines	LF, CC, and metaheuristic algorithms	HOMER + PSO + GA + grey wolf optimizer	Egypt	The grey wolf optimizer is more efficient than dispatch algorithms.

Numerous studies have adopted different custom control dispatch strategies for HESs with FCs using other simulation tools. Mukherjee et al. [26] used general algebraic modeling to conduct an economic analysis of a grid-connected PV-wind-FC system. However, the capital costs of individual components and grid-related constraints were not considered. Other authors [27] developed a PV-EL proton-exchange membrane (PEM) hybrid model for a simulation and feasibility study; however, economic analysis and control dispatch algorithms were not included. Chen et al. [28] used a novel predictive control dispatch model to investigate the optimal design of a grid-tied wind-hydrogen-FC system. It was found that the proposed methodology could maximize the local usage of wind power while minimizing the power exchange with the grid. Torreglosa et al. [29] presented a predictive control dispatch model to optimize the sizing of the PV, wind, FC, and BES system and maximize economic benefits. It was found that the proposed model achieved a low NPC while still satisfying the load demand. Abdelghany et al. [30] developed a new model predictive controller strategy for optimal operation of grid-connected wind farms using hydrogen-based energy storage systems and local loads. The results showed that the proposed control strategy minimizes switching among different operating modes of hydrogen storage and maximizes revenue through electricity market participation. Jamshidi et al. [31] proposed a multi-objective crow search algorithm to optimize and determine the economic viability of a PV, FC, EL, hydrogen tank (HT), and DG system. The results revealed that the proposed algorithm achieved a low NPC with high integration of hydrogen energy.

The literature survey indicates that LF and CC control dispatch algorithms are available, but the main problem with these control dispatch methods is their inability to optimally control the FC and enter the constraints and conditions related to the FC during the HOMER simulation [32]. In addition, CC and LF dispatch controls limited the utilization of a BES (CC control dispatch) or FC, which is frequently operated under partial load (LF control dispatch) [33]. Such suboptimal operation can affect the economic benefits of the microgrid system and the optimal design, and can increase the operating costs owing to the lower off-design efficiency. For both CC and LF strategies, HOMER computes the cost of discharging the BES, compares it with the cost of running the FC, and chooses the option

with the lowest cost that also meets the power demand at each time step [34]. Therefore, the control strategies in HOMER are considered economic dispatch strategies, taking the parameters that affect the economic state of the HES into consideration with a higher priority than the technical parameters. The major purpose of the technical parameters in HES is to increase the system performance, lifetimes of components, and stability of the system. Because the default dispatch strategies in HOMER have these limitations, an improved energy management algorithm is needed in HOMER to operate microgrid systems more optimally to prevent over- or under-utilization of the components and to minimize the NPC associated with microgrid power generation. Furthermore, custom control dispatch methods were shown to be able to optimize HESs, but improvements in energy management and FC operational considerations were not taken into account.

The motivation of this study was based on the need to develop a control dispatch strategy to thoroughly characterize and control the behavior of PVs, BESs, and FCs. More specifically, in this study, the energy management of HES was investigated to achieve optimal economic energy flow management. In the proposed dispatch (PD) strategy, the economic costs, technical parameters, and constraints of the PV-FC-BES system were also considered. The HES was modeled using a rule-based algorithm developed in MATLAB Version 2021a, Mathworks Inc., Natick, MA, USA. The PD strategy enables the determination of the optimal component sizes of the PV, BES, and FC, and guarantees that the FC is running whenever possible at the maximum rated capacity while remaining within the constraints. The PD strategy aims to overcome the limitations of the default LF and CC strategies in HOMER and improve the optimum microgrid sizing results. The main contributions of this study are as follows:

1. The development of a novel control dispatch model that controls the PV, BES, and FC arbitrarily during the optimization process and economically serves the load demand at the minimum NPC.
2. A hybrid analysis of the PV-FC-BES system, considering sizing optimization and energy management planning with the aim of increasing the FC capacity factor during FC operation.
3. Analysis of the benefits of the PD strategy versus LF and CC control dispatch, based on a case study of an off-grid zero-energy office building with 100% renewables.

The remainder of this paper is organized as follows. In Section 2, the renewable energy resources and load demand considerations are presented. Section 3 explains the mathematical modelling of the microgrid components. In Section 4, the PD strategy is compared with the existing LF and CC control strategies. Finally, Section 5 presents the conclusions.
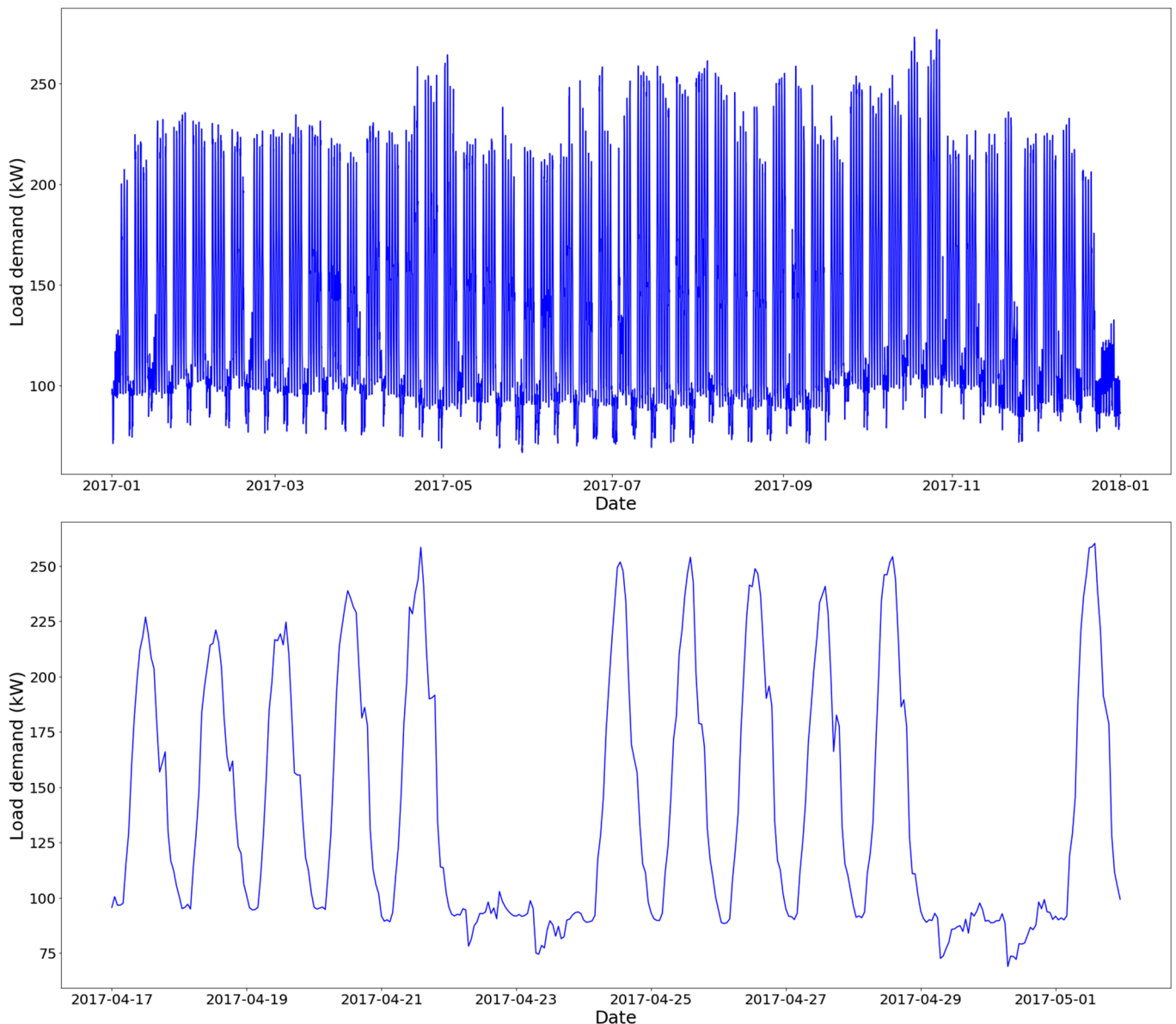
2. Renewable Energy Resources and Load Demand

2.1. Study Building

The present study was carried out at the Student Services Center building at the University of California, San Diego (UCSD) campus, at 9500 Gilman Dr, La Jolla, CA 92093, USA (32°52.8′ N, 117°14.0′ W). The building includes 135,085 ft^2 of gross floor area on five stories. It was constructed in 2007 and has a mean load of 140 kW.

2.2. Load

The total electric load at a resolution of 15 min for the Student Services Center building was obtained from an open-source database [35] (Figure 1). In this research, 8760 h time series load data were then inputted into HOMER to optimize the capacity of the microgrid system. The power demand is higher on weekdays than on weekends. The minimum and maximum loads were stable throughout the year, but the peak loads were higher in July through October.

Figure 1. Power demand data for the Student Services Center building for (**top**) the complete year dataset and (**bottom**) two weeks during the academic year.

2.3. Renewable Energy Resources

Solar irradiation is an important criterion for determining PV performance outcomes. This study used the global horizontal irradiance 8760 h time series as input in HOMER to design and model the HES. Figure 2 shows the average monthly solar irradiance data obtained from the NASA Weather Resource Data Center [36]. The daily average solar irradiation received in San Diego, California is relatively high at 5.0 kWh/m^2/day, making solar energy systems attractive energy sources.
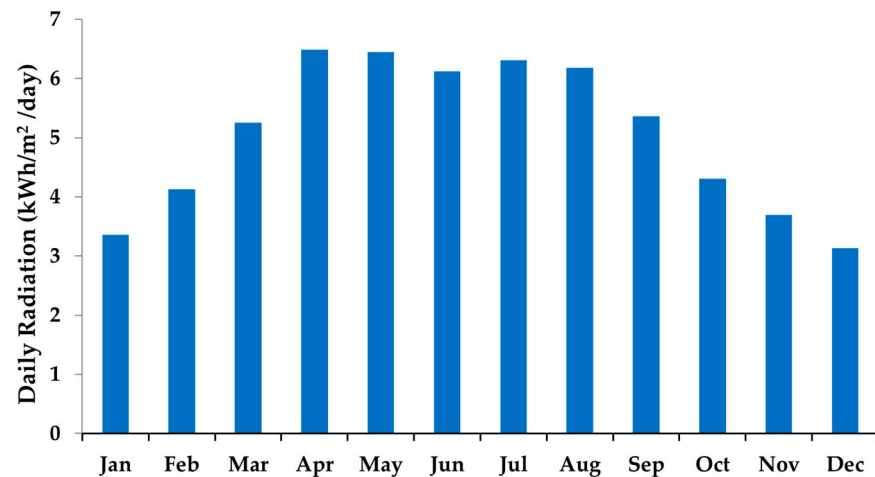
Figure 2. Annual cycle of monthly solar irradiance in San Diego.

3. Methodology

3.1. Overview

This study presents an optimal framework for the HES to satisfy the load demand. Figure 3 illustrates the interaction between HOMER and MATLAB, where the PD controls and coordinates the optimal dispatch of the HES. The final outputs are the optimal system sizes and minimum NPCs from all possible combinations of the HES. The main steps of the algorithm are as follows:

Step 1: System configuration. Load demand, component specifications, and meteorological data, such as solar irradiance data, are input into HOMER to optimize the microgrid system.

Step 2: Control dispatch. To use the MATLAB Link control dispatch, the MATLAB dispatch function is required, where we write our code (inputting rules and constraints) that defines the dispatch schedule. In this manner, we define our own strategies to prioritize FC power generation. In addition, no charging set point is considered, and the BES discharging operation is determined based on the BES capacity to supply the net required load after the FC power is exhausted, contrary to the CC and LF control dispatch. The implemented code aims to optimize the PV, FC, and BES and determine the system sizes with the minimum NPC that can reliably meet the power demand. During the simulation process, HOMER simulates the energy flow at the current time step according to the dispatch commands. MATLAB Link allows the PD strategy to more precisely control energy management by determining the dispatch priority of each component in the system.

Step 3: Simulation results. HOMER analyzes a set of different system configurations. In the enumerative optimization process, HOMER examines all possible combinations, discards infeasible options that are unable to meet the given constraints, and then displays a list of feasible options and sorts them according to the optimization variable of choice (NPC) [37].
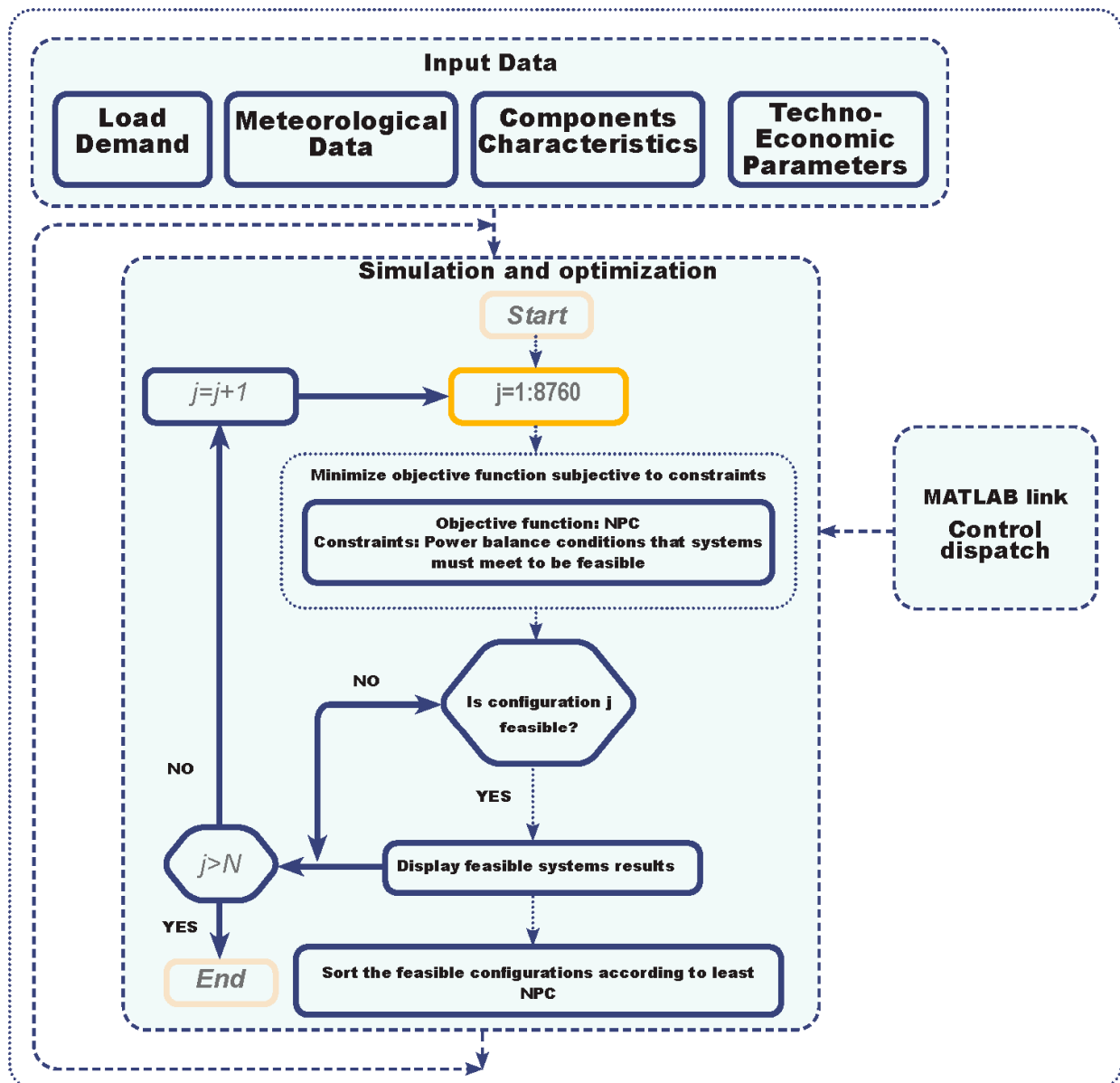
Figure 3. Flowchart of the analysis procedure.

3.2. System Design and Economic Components

The proposed HES consists of a PV, FC, BES, HT, and EL, as shown in Figure 4. The PV, FC, BES, and EL were linked to the DC bus, while the load demand was connected to the AC bus. The EL uses electricity from the PV panels to generate hydrogen, which is stored in the HT. However, the power electronics used to connect the system components were not considered in this study. The technical parameters and economic data were obtained from the literature [38–40] and are listed in Table 2. The project lifetime was assumed to be 25 years. An inflation rate of 2% and discount rate of 8% [36] were also assumed.

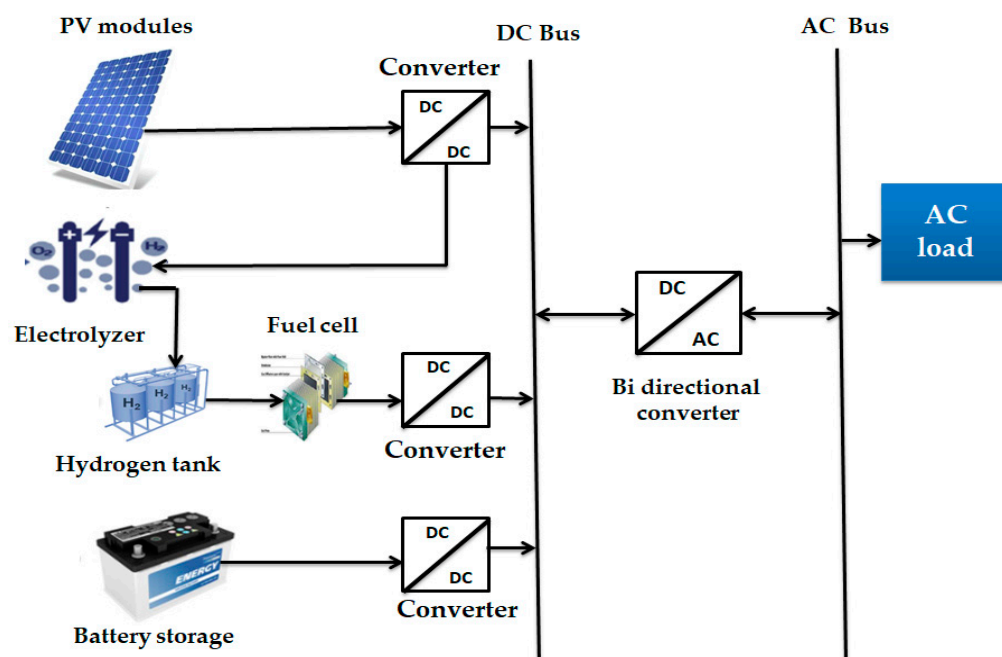**Figure 4.** Proposed HES.

Table 2. Capital (CAPEX) and operating and maintenance (OPEX) costs of different components.

Components	Lifetime (Years)	CAPEX ($/kW)	OPEX ($/kW)
PV	25	1720	2.5% of CAPEX
BES	15	700	3% of CAPEX
FC	7	2500	0.02
EL	15	2500	80
HT	15	1000	10

3.3. Models of Major Components

3.3.1. PV Modules

The PV power output is calculated based on irradiance and temperature values. An SPR-E20 monocrystalline silicon PV module was chosen for this study. The generated PV power is calculated as follows [41]:

$$\text{PV electricity production} = Y_{PV}\, f_{PV} \left(\frac{G_T}{G_{T,STC}} \right) [1 + K_P(T_c - T_{c,STC})] \qquad (1)$$

where Y_{PV} is the PV array power under standard test conditions (kW), f_{pv} is the derating factor (%), G_T is the incident plane of array solar irradiance (kW/m^2), $G_{T,STC}$ is the incident solar irradiance under standard test conditions (kW/m^2), T_c is the PV cell temperature (°C), $T_{c,STC}$ is the temperature under standard test conditions (25 °C), and K_P is the power temperature coefficient (%/°C).

3.3.2. Battery Energy Storage System (BES)

In HES, the BES supplies electricity during periods of relatively low renewable energy power production. In this study, the BES stores excess energy and supplies electricity when the FC and PV cannot satisfy the required load demand. The cost and performance parameters of lithium-ion BES technology were selected [42]. The charge and discharge powers of the BES depend on the SOC. The charging rate of the BES $P_b(t)$ is calculated using Equation (2) [43] where $Q_s(t)$ is the available energy at the beginning of the time step (kWh) and above the minimum state of charge level (SOC$_{min}$ = 20%), while the maximum state

of charge level SOC_{max} is 80%. The SOC was chosen based on the optimum charge range of the lithium-ion BES (for the lifespan). Q (t) is the total amount of energy [kWh] at the end of the time step, c is the storage capacity ratio (unitless), k is the storage rate constant (h^{-1}), and Δt is the time step size (h). The maximum BES discharge power $P_{b,max}(t)$ can be calculated using Equation (3) [43], where Q_{max} is the total storage capacity (kWh).

$$P_b(t) = \frac{kQ_s(t)e^{-k\Delta t} + Q(t)kc(1 - e^{-k\Delta t})}{1 - e^{-k\Delta t} + c(k\Delta t - 1 + e^{-k\Delta t})} \tag{2}$$

$$P_{b,max}(t) = \frac{-kcQ_{max} + kQ_s(t)e^{-k\Delta t} + Q(t)kc(1 - e^{-k\Delta t})}{1 - e^{-k\Delta t} + c(k\Delta t - 1 + e^{-k\Delta t})} \tag{3}$$

3.3.3. Fuel Cell Systems (FC)

Maximizing the FC capacity factor is the major objective of the PD strategy to examine the performance of the HES. A FC is an electrochemical engine that generates electricity through oxidation and reduction reactions in which hydrogen is oxidized without combustion and electricity is produced. To model a FC in HOMER, we added a generator, set the fuel to hydrogen, and adjusted the fuel curve to match the hydrogen FC specifications. The fuel curve describes the amount of hydrogen consumed by an FC system to produce electricity. We define the electrical efficiency of the FC as the electrical energy divided by the chemical energy of the entering fuel. The efficiency of FC (η_{FC}) is calculated using Equation (4) [44,45]:

$$\eta_{FC} = \frac{3600 \times P_{FC}}{F(t) \times LHV_H} \tag{4}$$

where P_{FC} is the FC output power (kW) and LHV_H is the lower heating value (a measure of energy content) of hydrogen [MJ/kg]. FCs and their components are primarily designed to operate in the high-load or power-range modes rather than in the continuous low-load mode. This means that the nominal efficiency of the FC experiences a significant drop in continuous low-load mode [44]. η_{FC} depends on the power output of the FC (P_{FC}), with an efficiency of 33.9% at the full-load demand level (P_{FC} = 100%), 28.2 % at a partial-load demand level of 50%, 18.8% at a low-partial-load level of 20%, and 7.0% at a low-partial-load level of 5% [45–47]. In this study, the electrolyzer efficiency was assumed to be 79%. The amount of hydrogen F(t) consumed to produce electricity is expressed as follows [45]:

$$F(t) = F_0 \cdot P_{FC} + F_1 \cdot P(t) \tag{5}$$

where F(t) is the mass of hydrogen used in FC (kg/h). P(t) is the output power of the FC at time t; F_0 is the fuel curve intercept coefficient (0.033 kg/h/kW); that is, the FC no-load consumption divided by the FC rated capacity; and F_1 is the fuel curve slope coefficient (0.273 kg/h/kW) [46]. These coefficients were obtained from the linear fuel consumption curve and assisted in the calculation of the hydrogen consumption rate at a particular time step.

3.4. Economic Indicators

The costs (LCOE and NPC) of the different optimized configurations of the HES were determined. The amount of the minimum NPC ($) can be acquired through the ratio of the total annualized cost (TAC) at the start of the project ($), which consists of the equipment cost, installation cost, operation costs, and replacement cost to the total recovery factor (CRF) [48]:

$$NPC = \frac{TAC}{CRF(i, n)} \tag{6}$$

where i is the annual real discount rate (%) and n is the project lifetime (years). CRF can be expressed as follows [49]:

$$CRF(i,n) = \frac{i(1+i)^n}{(1+i)^n - 1} \qquad (7)$$

The LCOE ($/kWh) is defined as the ratio of the sum of the total annualized cost to the yearly energy production [50,51]:

$$LCOE = \frac{TAC}{E_{served}} \qquad (8)$$

where E_{served} is the yearly total load served (kWh).

3.5. Formulation of the Optimization

Figure 5 shows a flowchart of the PD algorithm. The PD algorithm aims to satisfy the power demand while fulfilling the given constraints and minimizing the NPC. The optimization strategy is as follows:

Case 1. If the electricity generated from the PV exceeds the load requirement, the load is satisfied by the PV power output, and the excess electricity goes to the EL to produce hydrogen for storage in the HT. Otherwise, the excess electricity charges the BES. The FC remains off.

Case 2. If the load demand exceeds the PV power output and the PV power output is not zero (as in Case 3), the FC is turned on. The algorithm prioritizes PV and FC to satisfy the energy demand. There are two possible explanations for this case.

- The PV + FC can satisfy the load demand, and the remaining power to satisfy the load demand is provided by the FC. The minimum load ratio of the FC was set to 50% of its capacity to prevent the FC from operating under a low load with low efficiency. The authors [46] found that when the partial-load demand was larger than 51.1%, the electrical efficiency increased, whereas a low-partial load decreased the electrical efficiency. Therefore, if the required electricity from the FC is less than 50% of its capacity, then the FC operates at 50%. The difference between power generation and power demand is then $\Delta P(t) = \left(P_{PV(t)} + P_{FC(t)}\right) - P_{load(t)}$. If $\Delta P(t) > 0$, then the remaining power is fed to the EL ($P_{EL}(t) = \Delta P(t)$) to produce hydrogen for storage. If the power fed to the EL is greater than the power rating of the electrolyzer (P_{rEL}), the remaining power is used to charge the BES.
- The PV + FC cannot satisfy the load demand, that is, $P_{PV(t)} + P_{FC(t)} < P_{load(t)}$, so the FC runs at full-rated capacity (100%) and the BES supplements the remaining power to meet the energy demand; i.e., $P_{BES(t)} = P_{load(t)} - P_{PV(t)} - P_{FC(t)}$.

Case 3. At night, when the PV power output is zero, i.e., $P_{PV(t)} = 0$, the FC turns on at the full-rated capacity.

- If $P_{FC(t)} > P_{load(t)}$, the FC power output can satisfy all load demands, and the BES is not used.
- If the FC cannot satisfy the load demand, then the BES will assist in satisfying the load demand, that is, $P_{BES(t)} = P_{load(t)} - P_{FC(t)}$.

Case 4. If the power from the PV, FC, or BES cannot meet the load demand, that is, $P_{PV(t)} + P_{FC(t)} + P_{BES(t)} < P_{load(t)}$, the missing load is defined as the unmet load via $P_{Uload(t)} = P_{load(t)} - (P_{PV(t)} + P_{FC(t)} + P_{BES(t)})$. Similarly, excess energy is defined as the energy that cannot be directly used or stored in the BES or HT.
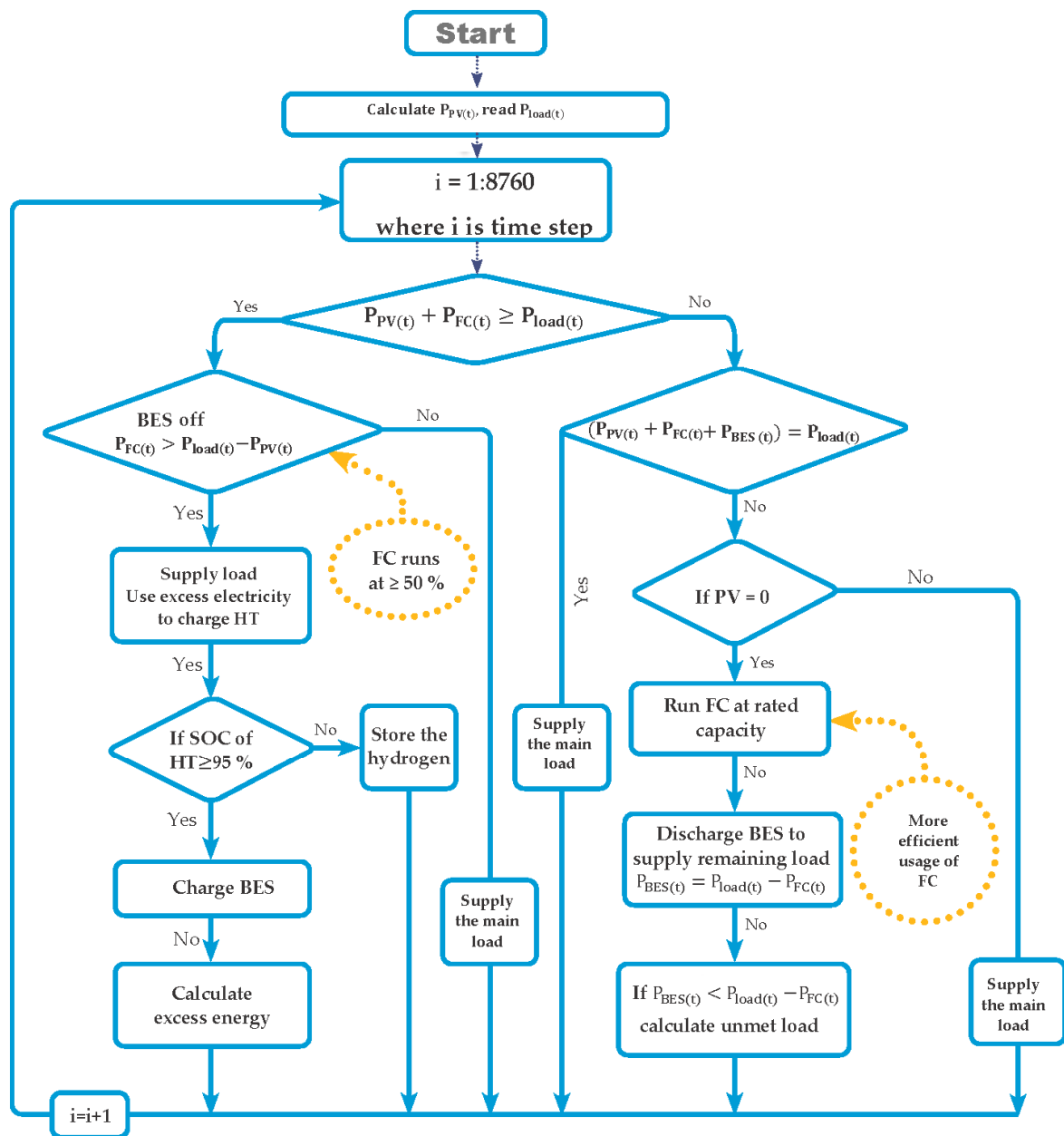
Figure 5. Control algorithm for PD strategy.

In the present study, to determine the economic viability of HES for the selected building, the minimum NPC outcomes were used as the objective function. The NPC is minimized through proper sizing (CAPEX) and utilization (OPEX) of each component. The objective function is expressed as [52]:

$$\text{Min(NPC)} = f(\text{PV}, \text{FC}, \text{BES}, \text{EL}, \text{HT}) \tag{9}$$

The system with the lowest NPC also possessed the lowest LCOE. The sizing consists of defining the installed capacities of the PV, FC, BES, EL, and HT, which are the decision

variables for this feasibility study. The decision variable constraints in the PD algorithm
are [53]:

$$\text{Constraints} \begin{cases} \text{SOC}_{\text{max}} \leq 80\% \\ \text{SOC}_{\text{min}} \geq 20\% \\ \text{FC}_{\text{LF}} \geq 50\% \\ \text{SOC}_{\text{H2-ST}}^{\text{min}} \geq 15\% \\ \text{SOC}_{\text{H2-ST}}^{\text{max}} \leq 95\% \end{cases} \tag{10}$$

where SOC is the BES state of charge, $\text{SOC}_{\text{H2-ST}}$ is HT state of charge, and FC_{LF} is the load
factor of the FC (%). To prevent the running of the FC with low efficiency, $\text{FC}_{\text{LF}} = 50\%$ was
imposed. A minimum SOC of 20% was set to avoid damage to the BES owing to excessive
discharge. The capacity constraints of the five decision variables (PV, FC, BES, EL, and
HT) are listed in Table 3. To determine the optimized solutions, HOMER performed more
than 25,000 simulations using different decision variables. Each simulation determined
the energy balance for each hour of the year, considering the optimization criteria and
constraints. During the simulation, HOMER called the PD algorithm at each time step.

Table 3. Capacity limits of optimization variables applied when minimizing the objective function in
Equation (9).

Components	Capacity Constraints
PV	$\leq$ 1500 kW
FC	$\leq$ 250 kW
BES	60 kWh $\leq$ BES $\leq$ 100 kWh
EL	$\leq$ 1450 kW
HT	1000 kg $\leq$ HT $\leq$ 1500 kg

## 4. Results and Discussion

In this section, we analyze the effects of three different control strategies (LF, CC, and
PD) on the economic and technical performance of the HES.

4.1. Economic Analysis

Different configurations of the HES were examined to identify the optimal configura-
tion with the minimum NPC. Each dispatch strategy creates different optimal combinations
of equipment size. The sizing and economic results for each dispatch algorithm are pre-
sented in Table 4 and Figure 6, respectively. The results reveal that the configuration with
the lowest NPC was obtained with the PD strategy, as the PV and BES system sizes required
by the PD strategy are smaller than those in the existing control strategies. The PD strategy
also had a lower PV capacity (1100 kW) than the PV capacity of the LF dispatch strategy
(1300 kW) and CC dispatch strategy (1350 kW). LF and CC yielded similar sizes of the
BES (80 kWh and 90 kWh) and FC (205 kW), whereas PD reduced the required capacity
of the BES to 70 kWh and reduced the capacity of the FC to 180 kW. It is evident that the
LCOE calculated in the PD strategy provided a smaller value than that of the existing
control strategies because it had the smallest CAPEX and OPEX values compared to the
HOMER control dispatch outcomes (Figure 6). The LCOE of the LF and CC strategies
were calculated to be higher ($0.590/kWh and $0.592/kWh, respectively) compared to
the PD strategy ($0.570/kWh), while the CC dispatch strategy had the highest LCOE of
0.592 $/kWh, which is 3.7% higher than that in the PD case. Moreover, the differences in
LCOE between the LF and CC dispatch strategies were negligible.

Table 4. Optimization results of LF, CC, and PD control strategies.

Components	Control Strategies		
	LF	**CC**	**PD**
PV (kW)	1300	1350	1100
BES (kWh)	90	80	70
FC (kW)	205	205	180
EL (kW)	1200	1200	1200
HT (kg)	1200	1200	1200
NPC (million $)	10.7	10.8	10.3
LCOE ($/kWh)	0.590	0.592	0.570
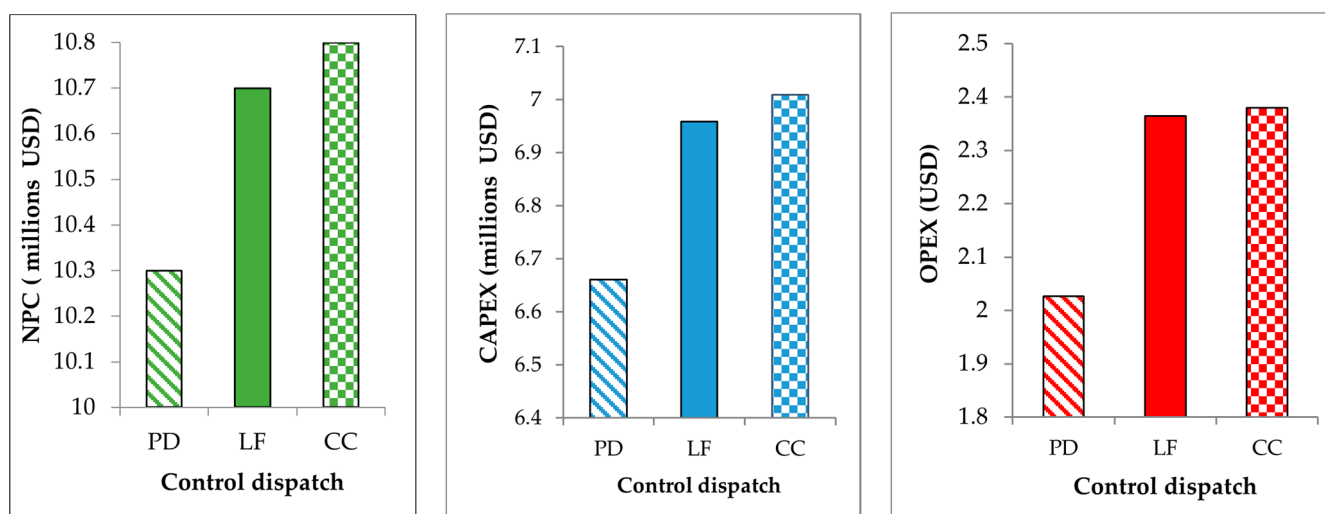
Figure 6. Net present cost, CAPEX, and OPEX for PD, LF, and CC control dispatch.

It is shown in Figure 6 that the PD strategy had a lower NPC ($10.3 M) compared to the NPC of the LF dispatch strategy ($10.7 M) and the CC dispatch strategy ($10.8 M). The higher costs of LF and CC are due to the larger sizes of the PV, BES, and FC components. These results demonstrate that the PD strategy obtained more economical dispatch decisions than the CC and LF control strategies. It is evident that the PD had the lowest CAPEX and lowest OPEX, yielding the lowest NPC. Because all OPEX costs are a function of the system size, it is trivial that a lower CAPEX occurs along with a lower OPEX.

4.2. Performance Analysis

Table 5 shows the yearly electrical production of each component and a comparison of the CC, LF, and PD control strategies (with percentage errors for each). It is clear that PV panels provided the largest share of electricity supply among the three different control dispatches. It is also evident that the electricity production from PV was 81.4% and 81.8% for LF and CC, respectively, whereas for PD, PV generated 76.3% of the total energy produced. A PV generates excess energy during periods of high irradiance. The addition of HT and BES provides the possibility of storing energy during the day and releasing it at night when no sunlight is available. As indicated in Table 5, the FC in PD contributed approximately 23.7% of the total electricity production, which was higher than that of the CC (18.2%) and LF (18.6%) strategies. It was observed that the PD strategy had a larger percentage as it aims to increase the operation of the FC as much as possible; hence, the electricity energy output from the FC was also increased. In addition, the energy production by the BES was relatively low (0.0%) in the CC, LF, and PD strategies.

Table 5. Electricity production results for one year for the LF, CC, and PD dispatch strategies.

Components	LF		CC		PD		% Errors (PD versus LF Control Dispatch)	% Errors (PD versus CC Control Dispatch)
	kWh/Year	%	kWh/Year	%	kWh/Year	%		
PV	2,274,113	81.4	2,361,579	81.8	1,924,250	76.3	−6.68	−6.55
FC	520,310	18.6	525,798	18.2	589,016	23.7	18.56	23.20
BES	7550		7917		4833		−56.21	−63.81
Unmet load (%)	0.433		0.306		0.050		−7.66	−5.12
FC run time (hours)	4871		4913		5312		8.30	7.51
Average SOC of BES (%)	92.81		98.26		98.14		5.43	−0.12

According to the results, FC in PD had the highest number of operating hours per year (5312 h/year), followed by CC (4913 h/year) and LF (4871 h/year). The capacity factor is the ratio of the actual electrical energy output over a given period to the maximum possible electrical energy output over that period. It is evident that the FC capacity factor was higher in PD (32.7%) than in LF (29.0%) and CC (29.2%). This result can be explained by the fact that PD overcomes the limitations of LF and CC by exploiting more FC power to supply the load demand. The proper distribution of electricity production among the components leads to a reduction in the unmet load and the BES capacity. It is clear that PD was more effective in managing the power flow to reduce the unmet load by only 0.050%, followed by the CC (0.306%) and LF (0.433%) strategies. It was also observed that PD outperformed LF and CC control dispatches on all economic and reliability metrics.

The annual energy throughput is the total amount of energy, in watt-hours, that a BES can be expected to store and deliver in one year. It is clear that the PD strategy had the lowest input and output energy of the BES (5310/4833 kWh), followed by the LF (8447/7550 kWh) and CC (8861/7917 kWh) strategies. This result is mainly due to the fact that in LF, the FC only generates sufficient power to satisfy the load and does not charge the BES, resulting in low charge and discharge cycles. Conversely, in the CC, the FC system charges the BES whenever it runs. For the LF and CC control strategies, there was a noticeable difference owing to the operation of the FC and BES. For example, for LF, higher PV and BES capacities were required because of the limitation of the BES and FC operation, which provides sufficient power to meet the power demand.

Table 6 summarizes the key qualitative differences between the three control strategies. There was a noticeable difference in the NPC, LCOE, and FC operation owing to the oversizing of microgrid components and the poor management of the power flow in the default HOMER control strategies LF and CC. As indicated in Table 4, the PD case offers attractive technical and economic performance because it had the lowest NPC and LCOE. Thus, the PD is a promising strategy for controlling the energy management in microgrid systems by improving the effective utilization of FC systems. However, this study had a limitation regarding the sensitivity analysis of the input parameters of the LCOE and NPC.

Table 6. Overview of the key differences between CC, LF, and PD approaches.

Criterion	CC	LF	PD
BES utilization	-BES is only discharged if it was discharged in the previous time step or it is at maximum SOC.	-BES is allowed to discharge energy while the FC is supplying the load.	-PD does not decide the BES discharging operation based on BES's maximum SOC, or charge/discharge status of the previous time step. -BES discharging operation is determined based on the BES's capacity to supply the net required load after the FC power has been exhausted.
FC operation	-FC operates at full-rated power to meet power demand. -When the FC runs, excess FC energy is used to charge the BES.	-FC works frequently at partial load. -BES is only charged from PV systems. -FC never charges BES.	-Higher operational efficiency of FC by operating FC only at 50% capacity or more. -The BES is charged with surplus FC energy.

Table 6. *Cont.*

Criterion	CC	LF	PD
Optimization process	Single objective optimization. At each time step, the decision to use the FC or the BES is made based on the lowest-cost choice. The technical performances are not taken into the higher priority in finding the optimal design.	Same as CC	Multi-objective techniques. Combine technical parameters and economic control strategy to increase the system performance, components lifetime, and system stability achieve synergy between the lowest NPC of microgrid system and coordinated control of PV/FC/BES devices.

4.3. Comparison to Systems in the Literature

Table 7 presents the economic results of several studies that used different dispatch strategies. In most of these studies, custom dispatch strategies provided economic benefits over default HOMER control strategies. In this study, the advantage of the PD is its ability to increase system performance outcomes and reduce the unmet load in off-grid systems. In addition, none of these studies increased the operation of the FC in a HES.

Table 7. Comparative analysis with the similar relevant study of recent study.

Reference/Year	Location	Components	Dispatch Strategy	LCOE ($/kWh)	Percentage of Renewable Energy (%)
Jufri et al. [54], 2021	Indonesia	PV/BES	HOMER Optimal BES	0.19 0.18	22.4 34.0
Toopshekan et al. [55], 2020	Iran	PV/wind/DG/BES/grid	HOMER Predictive dispatch	0.13 0.12	37.0 46.4
Cano et al. [56], 2021	Galapagos Islands	PV, BES, DG, wind turbines, hydraulic pumping	HOMER SDO	0.25 0.26	74.3 74.3
Our findings	USA	PV/FC/BES	HOMER PD strategy	0.59 0.57	100 100

5. Conclusions

Control dispatch strategies are critical in assessing the feasibility and performance of HESs. In this study, a novel control dispatch strategy was developed for a PV-FC-BES system using MATLAB software. We implemented a dispatch algorithm, the goal of which was to minimize the NPC by maximizing the use of FC systems with optimal management of the power flow between the PV, BES, and FC. The PD strategy allows the optimization of project lifetime costs under the given constraints. A cost-effective HES was designed by properly sizing the components and devising an efficient control dispatch strategy. Three operational strategies were compared in terms of their techno-economic performance capabilities. Based on the results, the PD algorithm was proven to be superior for the economic optimization of the HES. The main findings are as follows.

- The PD strategy met the load demand with more reliable optimization results than the CC and LF control dispatches. Furthermore, the PD was found to be the most feasible and cost-effective compared to LF and CC dispatches, as the prioritization of the energy supply between the PV, BES, and FC was managed more effectively than in the LF and CC cases.
- The PD strategy presented in this study reduced the NPC by increasing the operation of the FC compared to CC and LF, both in terms of hours and capacity factor. Therefore, the PD strategy can promote FC systems and a solar-based 100% renewable energy supply in an off-grid system.

These outcomes are relevant to those who make investment decisions related to the supply of electricity to office buildings using renewable energy systems, and support

the implementation of such systems in remote areas. In addition, this study could be instrumental for companies, policymakers, and governments to implement superior energy management strategies in other remote areas to reduce their dependence on the electric grid. Furthermore, the proposed dispatch strategy can help improve the cost competitiveness of renewable energy systems. Based on this study, it is crucial to continue developing control dispatch strategies that should be applied to actual microgrid systems to expand the use of microgrid systems.

Author Contributions: Conceptualization, L.U.; Methodology, L.U.; Simulation, L.U.; Resources, H.-G.K., J.K. and C.K.K.; Validation, J.K.; writing-original draft preparation, L.U.; Supervision, H.-G.K. and J.K. All authors have read and agreed to the published version of the manuscript.

Institutional Review Board Statement: Not applicable.

Informed Consent Statement: Not applicable.

Data Availability Statement: All data are available in the paper.

Nomenclature

AC	Alternating current
BES	Battery energy storage system
c	Storage capacity ratio
CAPEX	Capital cost
CC	Cycle-charging
CRF	Capacity recovery factor
DC	Direct current
DG	Diesel generator
E_{FC}	Output energy of the fuel cell component
EL	Electrolysis
FC	Fuel cell system
FC_{LF}	Load factor of fuel cell
F_0	Co-efficient due to the fuel curve intercepts
F_1	Slope of the hydrogen curve
F(t)	Mass of hydrogen used in the fuel cell in relation to the electricity output
f_{pv}	Derating factor
GA	Genetic algorithm
G_T	Incident plane of array solar irradiance
$G_{T,STC}$	Incident solar irradiance under test conditions.
HES	Hybrid energy system
HOMER	Hybrid Optimization of Multiple Energy Resources
HT	Hydrogen tank
i	Annual real discount rate
k	Storage rate constant
K_P	Power temperature coefficient
LCOE	Levelized cost of energy
LF	Load-following
Min	Minimum
MOPSO	Multi-objective particle swarm optimization
NASA	National Aeronautics and Space Administration
n	Project lifetime
η_{FC}	Efficiency of fuel cell system
OPEX	Operational and maintenance cost
NPC	Net present cost

PD	Proposed dispatch
P_{FC}	Rated output power of fuel cell
PSO	Particle swarm optimization
PV	Photovoltaic system
P_{rEL}	Power rating of electrolyzer
$P_{Uload(t)}$	Unmet power demand
P(t)	Output power of fuel cell
Q(t)	Total amount of energy at the beginning of the time step
Q_{max}	Total storage capacity
$Q_s(t)$	Available energy at the beginning of the time step
SOC	State of charge
SDO	Simulink design optimization
SOC_{H2-ST}	State of charge of hydrogen storage system
t	Time
TAC	Total annualized cost
T_c	Photovoltaic cell temperature
$T_{c,STC}$	Temperature at standard test conditions
UCSD	University of California, San Diego
Y_{PV}	Photovoltaic array power at standard test conditions

References

1. Shan, Y.; Guan, D.; Liu, J.; Mi, Z.; Liu, Z.; Liu, J.; Schroeder, H.; Cai, B.; Chen, Y.; Shao, S.; et al. Methodology and applications of city level CO_2 emission accounts in China. *J. Clean. Prod.* **2017**, *161*, 1215–1225. [CrossRef]
2. Shin, H.K.; Cho, J.M.; Lee, E.B. Electrical Power Characteristics and Economic Analysis of Distributed Generation System Using Renewable Energy: Applied to Iron and Steel Plants. *Sustainability* **2019**, *11*, 6199. [CrossRef]
3. Mengelkamp, E.; Gärttner, J.; Rock, K.; Kessler, S.; Orsini, L.; Weinhardt, C. Designing microgrid energy markets: A case study: The Brooklyn Microgrid. *Appl. Energy* **2018**, *210*, 870–880. [CrossRef]
4. Mehrpooya, M.; Ghorbani, B.; Mousavi, S.A. Integrated power generation cycle (Kalina cycle) with auxiliary heater and PCM energy storage. *Energy Convers. Manag.* **2018**, *177*, 453–467. [CrossRef]
5. Al Mouatamid, A.; Ouladsine, R.; Bakhouya, M.; El Kamoun, N.; Khaidar, M.; Zine-Dine, K. Review of Control and Energy Management Approaches in Micro-Grid Systems. *Energies* **2021**, *14*, 168. [CrossRef]
6. Brenna, M.; Foiadelli, F.; Longo, M.; Abegaz, T. Integration and optimization of renewables and storages for rural electrification. *Sustainability* **2016**, *8*, 982. [CrossRef]
7. Jiang, F.; Xie, H.; Ellen, O. Hybrid energy system with optimized storage for improvement of sustainability in a small town. *Sustainability* **2018**, *10*, 2034. [CrossRef]
8. Mazzola, S.; Astolfi, M.; Macchi, E. A detailed model for the optimal management of a multi good microgrid. *Appl. Energy* **2015**, *154*, 862–873. [CrossRef]
9. Chauhan, A.; Upadhyay, S.; Khan, M.; Hussain, S.M.; Ustun, T.S. Performance Investigation of a Solar Photovoltaic/Diesel Generator Based Hybrid System with Cycle Charging Strategy Using BBO Algorithm. *Sustainability* **2021**, *13*, 8048. [CrossRef]
10. Dawood, F.; Shafiullah, G.M.; Anda, M. Stand-alone microgrid with 100% renewable energy: A case study with hybrid solar PV-battery-hydrogen. *Sustainability* **2020**, *12*, 2047. [CrossRef]
11. Singh, A.; Baredar, P.; Gupta, B. Techno-economic feasibility analysis of hydrogen fuel cell and solar photovoltaic hybrid renewable energy system for academic research building. *Energy Convers. Manag.* **2017**, *145*, 398–414. [CrossRef]
12. Ghenai, C.; Bettayeb, M. Optimized design and control of an off grid solar PV/hydrogen fuel cell power system for green buildings. *IOP Conf. Ser. Earth Environ. Sci.* **2017**, *93*, 012073. [CrossRef]
13. Kansara, B.U.; Parekh, B.R. Penetration of renewable energy resources based dispatch strategies for isolated hybrid systems. *Int. J. Electr. Electron. Eng. Res.* **2013**, *3*, 121–130.
14. Arévalo, P.; Benavides, D.; Lata-García, J.; Jurado, F. Techno-economic evaluation of renewable energy systems combining PV-WT-HKT sources: Effects of energy management under Ecuadorian conditions. *Int. Trans. Electr. Energy Syst.* **2020**, *30*, e12567. [CrossRef]
15. Shoeb, M.; Shafiullah, G. Renewable energy integrated islanded microgrid for sustainable irrigation—A Bangladesh perspective. *Energies* **2018**, *11*, 1283. [CrossRef]
16. Arévalo, P.; Jurado, F. Performance analysis of a PV/HKT/WT/DG hybrid autonomous grid. *Electr. Eng.* **2021**, *103*, 227–244. [CrossRef]
17. Rezzouk, H.; Mellit, A. Feasibility study and sensitivity analysis of a stand-alone photovoltaic diesel battery hybrid energy system in the north of Algeria. *Renew. Sustain. Energy Rev.* **2015**, *43*, 1134–1150. [CrossRef]
18. Yilmaz, S.; Dincer, F. Optimal design of hybrid PV-Diesel-Battery systems for isolated lands: A case study for Kilis, Turkey. *Renew. Sustain. Energy Rev.* **2017**, *77*, 344–352. [CrossRef]

19. Rajbongshi, R.; Borgohain, D.; Mahapatra, S. Optimization of PV-biomass-diesel and grid base hybrid energy systems for rural electrification by using HOMER. *Energy* **2017**, *126*, 461–474. [CrossRef]

20. Rashid, F.; Hoque, M.; Aziz, M.; Sakib, T.N.; Islam, M.; Robin, R.M. Investigation of Optimal Hybrid Energy Systems Using Available Energy Sources in a Rural Area of Bangladesh. *Energies* **2021**, *14*, 5794. [CrossRef]

21. Arévalo, P.; Benavides, D.; Lata-García, J.; Jurado, F. Energy control and size optimization of a hybrid system (photovoltaic-hydrokinetic) using various storage technologies. *Sustain. Cities Soc.* **2020**, *52*, 101773. [CrossRef]

22. Ghorbani, N.; Kasaeian, A.; Toopshekan, A.; Bahrami, L.; Maghami, A. Optimizing a hybrid wind-PV-battery system using GA-PSO and MOPSO for reducing cost and increasing reliability. *Energy* **2018**, *154*, 581–591. [CrossRef]

23. Fodhil, F.; Hamidat, A.; Nadjemi, O. Potential, optimization and sensitivity analysis of photovoltaic-diesel-battery hybrid energy system for rural electrification in Algeria. *Energy* **2019**, *169*, 613–624. [CrossRef]

24. Arévalo, P.; Eras-Almeida, A.A.; Cano, A.; Jurado, F.; Egido-Aguilera, M.A. Planning of electrical energy for the Galapagos Islands using different renewable energy technologies. *Electr. Power Syst. Res.* **2022**, *203*, 107660. [CrossRef]

25. Emad, D.; El-Hameed, M.A.; El-Fergany, A.A. Optimal techno-economic design of hybrid PV/wind system comprising battery energy storage: Case study for a remote area. *Energy Convers. Manag.* **2021**, *249*, 114847. [CrossRef]

26. Mukherjee, U.; Maroufmashat, A.; Ranisau, J.; Barbouti, M.; Trainor, A.; Juthani, N.; El-Shayeb, H.; Fowler, M. Techno-economic, environmental, and safety assessment of hydrogen powered community microgrids; case study in Canada. *Int. J. Hydrogen Energy* **2017**, *42*, 14333–14349. [CrossRef]

27. Kim, C.K.; Cho, H.S.; Kim, C.H.; Cho, W.; Kim, H.G. A Feasibility Study of Photovoltaic—Electrolysis—PEM Hybrid System Integrated Into the Electric Grid System Over the Korean Peninsula. *Front. Chem.* **2021**, *9*, 750. [CrossRef]

28. Chen, X.; Cao, W.; Zhang, Q.; Hu, S.; Zhang, J. Artificial intelligence-aided model predictive control for a grid-tied wind-hydrogen-fuel cell system. *IEEE Access* **2020**, *8*, 92418–92430. [CrossRef]

29. Torreglosa, J.P.; García, P.; Fernández, L.M.; Jurado, F. Energy dispatching based on predictive controller of an off-grid wind turbine/photovoltaic/hydrogen/battery hybrid system. Renew. *Energy* **2015**, *74*, 326–336.

30. Abdelghany, M.B.; Shehzad, M.F.; Liuzza, D.; Mariani, V.; Glielmo, L. Optimal operations for hydrogen-based energy storage systems in wind farms via model predictive control. *Int. J. Hydrogen Energy* **2021**, *46*, 29297–29313. [CrossRef]

31. Jamshidi, M.; Askarzadeh, A. Techno-economic analysis and size optimization of an off-grid hybrid photovoltaic, fuel cell and diesel generator system. *Sustain. Cities Soc.* **2019**, *44*, 310–320. [CrossRef]

32. Sánchez-Sáinz, H.; García-Vázquez, C.A.; Llorens Iborra, F.; Fernández-Ramírez, L.M. Methodology for the optimal design of a hybrid charging station of electric and fuel cell vehicles supplied by renewable energies and an energy storage system. *Sustainability* **2019**, *11*, 5743. [CrossRef]

33. Kansara, B.U.; Parekh, B.R. Dispatch, control strategies and emissions for isolated wind-diesel hybrid power system. *Int. J. Innov. Technol. Explor. Eng.* **2013**, *2*, 152–156.

34. Eu-Tjin, C.; Huat, C.K.; Seng, L.Y. Control strategies in energy storage system for standalone power systems. In Proceedings of the 4th IET Clean Energy and Technology Conference, Kuala Lumpur, Malaysia, 14–15 November 2016.

35. Silwal, S.; Mullican, C.; Chen, Y.A.; Ghosh, A.; Dilliott, J.; Kleissl, J. Open-source multi-year power generation, consumption, and storage data in a microgrid. *J. Renew. Sustain. Energy* **2021**, *13*, 025301. [CrossRef]

36. Monteiro, L.A.; Sentelhas, P.C.; Pedra, G.U. Assessment of NASA/POWER satellite-based weather system for Brazilian conditions and its impact on sugarcane yield simulation. *Int. J. Climatol.* **2018**, *38*, 1571–1581. [CrossRef]

37. Bahramara, S.; Moghaddam, M.P.; Haghifam, M.R. Optimal planning of hybrid renewable energy systems using HOMER: A review. *Renew. Sustain. Energy Rev.* **2016**, *62*, 609–620. [CrossRef]

38. Anoune, K.; Bouya, M.; Astito, A.; Abdellah, A.B. Sizing methods and optimization techniques for PV-wind based hybrid renewable energy system: A review. *Renew. Sustain. Energy Rev.* **2018**, *93*, 652–673. [CrossRef]

39. Al Garni, H.Z.; Awasthi, A.; Ramli, M.A. Optimal design and analysis of grid-connected photovoltaic under different tracking systems using HOMER. *Energy Convers. Manag.* **2018**, *155*, 42–57. [CrossRef]

40. Luta, D.N.; Raji, A.K. Optimal sizing of hybrid fuel cell-supercapacitor storage system for off-grid renewable applications. *Energy* **2019**, *166*, 530–540. [CrossRef]

41. Mamaghani, A.H.; Escandon, S.A.A.; Najafi, B.; Shirazi, A.; Rinaldi, F. Techno-economic feasibility of photovoltaic, wind, diesel and hybrid electrification systems for off-grid rural electrification in Colombia. *Renew. Energy* **2016**, *97*, 293–305. [CrossRef]

42. Das, B.K.; Alotaibi, M.A.; Das, P.; Islam, M.S.; Das, S.K.; Hossain, M.A. Feasibility and techno-economic analysis of stand-alone and grid-connected PV/wind/diesel/Batt hybrid energy system: A case study. *Energy Strategy Rev.* **2021**, *37*, 100673. [CrossRef]

43. Baneshi, M.; Hadianfard, F. Techno-economic feasibility of hybrid diesel/PV/wind/battery electricity generation systems for non-residential large electricity consumers under southern Iran climate conditions. *Energy Convers. Manag.* **2016**, *127*, 233–244. [CrossRef]

44. Thorstensen, B. A parametric study of fuel cell system efficiency under full and part load operation. *J. Power Sources* **2001**, *92*, 9–16. [CrossRef]

45. Getting Started Guide for HOMER (Version 2.8). Available online: https://www.homerenergy.com/products/pro/docs/latest/how_homer_creates_the_generator_efficiency_curve.html (accessed on 14 February 2022).

46. Liu, J.; Kim, S.C.; Shin, K.Y. Feasibility Study and Economic Analysis of a Fuel-Cell-Based CHP System for a Comprehensive Sports Center with an Indoor Swimming Pool. *Energies* **2021**, *14*, 6625. [CrossRef]

47. Stiel, A.; Skyllas-Kazacos, M. Feasibility study of energy storage systems in wind/diesel applications using the HOMER model. *Appl. Sci.* **2012**, *2*, 726–737. [CrossRef]
48. Masrur, H.; Howlader, H.O.R.; Elsayed Lotfy, M.; Khan, K.R.; Guerrero, J.M.; Senjyu, T. Analysis of techno-economic-environmental suitability of an isolated microgrid system located in a remote island of bangladesh. *Sustainability* **2020**, *12*, 2880. [CrossRef]
49. Ghenai, C.; Bettayeb, M. Modelling and performance analysis of a stand-alone hybrid solar PV/Fuel Cell/Diesel Generator power system for university building. *Energy* **2019**, *171*, 180–189. [CrossRef]
50. Mandal, S.; Das, B.K.; Hoque, N. Optimum sizing of a stand-alone hybrid energy system for rural electrification in Bangladesh. *J. Clean. Prod.* **2018**, *200*, 12–27. [CrossRef]
51. Ajlan, A.; Tan, C.W.; Abdilahi, A.M. Assessment of environmental and economic perspectives for renewable-based hybrid power system in Yemen. *Renew. Sustain. Energy Rev.* **2017**, *75*, 559–570. [CrossRef]
52. Rosenstiel, A.; Monnerie, N.; Dersch, J.; Roeb, M.; Pitz-Paal, R.; Sattler, C. Electrochemical Hydrogen Production Powered by PV/CSP Hybrid Power Plants: A Modelling Approach for Cost Optimal System Design. *Energies* **2021**, *14*, 3437. [CrossRef]
53. Quitoras, M.R.; Campana, P.E.; Rowley, P.; Crawford, C. Remote community integrated energy system optimization including building enclosure improvements and quantitative energy trilemma metrics. *Appl. Energy* **2020**, *267*, 115017. [CrossRef]
54. Jufri, F.H.; Aryani, D.R.; Garniwa, I.; Sudiarto, B. Optimal Battery Energy Storage Dispatch Strategy for Small-Scale Isolated Hybrid Renewable Energy System with Different Load Profile Patterns. *Energies* **2021**, *14*, 3139. [CrossRef]
55. Toopshekan, A.; Yousefi, H.; Astaraei, F.R. Technical, economic, and performance analysis of a hybrid energy system using a novel dispatch strategy. *Energy* **2020**, *213*, 118850. [CrossRef]
56. Cano, A.; Arévalo, P.; Jurado, F. A comparison of sizing methods for a long-term renewable hybrid system. Case study: Galapagos Islands 2031. *Sustain. Energy Fuels* **2021**, *5*, 1548–1566. [CrossRef]